Symposium on Applied Aerodynamics and Design of Aerospace Vehicle (SAROD 2024)
Month xx-xx, 2024, Thiruvananthapuram, India

Numerical Simulation of High–Speed Compressible Flow over Re-entry Vehicles using the OpenFOAM

Ishar Singh Saini[1], Biraj Khadka[2], Tushar Chourushi[3 *]

[1] Department of Aerospace Engineering, Amity University Mumbai, Panvel, Maharashtra, India
[2] Research Associate, FOSSEE, IIT Bombay, Mumbai, Maharashtra, India
[3,*]Department of Aerospace Engineering, MIT Art, Design and Technology University, Pune, Maharashtra, India

[3,*]Corresponding author: tushar.chourushi@mituniversity.edu.in

ABSTRACT

This project aims to simulate the supersonic/hypersonic flow over some blunt bodies using the sonicFoam solver which is part of the open-source software OpenFOAM and verify the obtained aerodynamic forces with the available results. The use of a blunt shape considerably reduces aero heating over the missiles and blunt shaped bodies but leads to increased drag which is quite useful when during a re-entry from space. The experimental results for bow-shocks of Kim, Chul-Soo [1] for a cylindrical body were validated in this study. Post validation, re-entry geometries which were taken from cases run by R.C. Mehta [2] [4] [5] are introduced in the flow and the aerodynamic parameters were calculated. Standard atmospheric values are used for air at sea level and varying the Mach numbers.

Keywords: CFD, hypersonics, aerodynamics, re-entry

NOMENCLATURE

L/D	Aspect Ratio	--
D	Diameter	[m]
C_D	Drag coefficient	--
U	Free-stream velocity	[m/s]
ρ	Density of air	[kg/m^3]
p	Pressure	[N/m^2]

1. INTRODUCTION

Re-entry bodies, such as space capsules and hypersonic vehicles, experience extreme thermal and aerodynamic loads as they re-enter a planetary atmosphere. This project aims to simulate the supersonic/hypersonic flow over some blunt bodies using the sonicFoam solver which is part of the open-source software OpenFOAM and verify the obtained aerodynamic forces with the available results. Using a blunt shape is found to considerably reduce aero heating over the missiles and blunt-shaped bodies but leads to increased drag, which is quite useful during re-entry from space, which is in agreement with the literature. The OpenFOAM code is validated with the experimental results of Kim, Chul-Soo [1] for a cylindrical body. Post validation, re-entry geometries which were taken similar to the cases of R.C. Mehta [2] are introduced in the flow and the aerodynamic parameters were calculated. Standard atmospheric values are used for air at sea level with varying Mach numbers.

2. OBJECTIVES

The study focuses on validating a supersonic flow over a 2D cylinder (D – 1m) by considering the fluid properties under a continuum regime, to simulate the flow over re-entry bodies. In the past, Kim, and Chul-Soo [1] performed experimental studies in a shock tube to determine the shape of detached shocks from a circular cylinder for a range of Mach numbers. Their results showcased an important key point: Two dimensionality is obtained at aspect ratio (L/D) which is greater than 5.5 for a Mach number range of 2.7 to 6.0. In this study, we try to validate these results and show the comparison of shock structure in this Mach number range. Figure 1 shows the visualization of two-dimensionality caused as the L/D is increased.

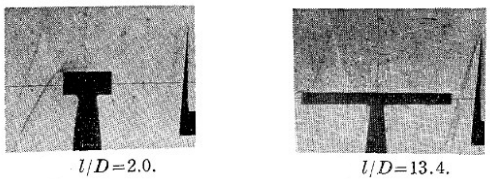

Fig 1. Visualization of shock wave over a circular cylinder in a shock tube (Reference figure taken from: *Experimental Studies of Supersonic Flow past a Circular Cylinder*", Kim, Chul-Soo [1])

Additionally, R.C. Mehta [2] showed a numerical study of the heat transfer and aerodynamic forces over various re-entry configurations by solving time-dependent compressible laminar Navier-Stokes equations and the results showcase comparisons of the flow field, surface pressure distribution and wall heat flux results are made between different configurations of the re-entry capsules with freestream Mach number 5 and standard air conditions at 29 km altitude. We implement the re-entry capsules of Apollo, ARD (ESA's Atmospheric Re-entry Demonstrator) and OREX (Orbital Re-entry Experiments).

3. METHODOLOGY

3.1. Solver Setup

The computational solving used the existing SonicFoam solver, a transient pressure-based solver for the trans-sonic/supersonic, turbulent flow of a compressible gas which is part of OpenFOAM v2212. It employs the PIMPLE algorithm, combining PISO and SIMPLE methods. The flow regime is governed by compressible Navier-Stokes equations and the Standard K-epsilon turbulence model with isothermal no slip wall condition. The postprocessing was done using Paraview v5.6.3. Computational resource utilized 8 parallel processing cores of processor over a Ram of 48 GB and Each simulation approximately took 30000 seconds to reach a steady state. The flow domain with the dimensions for the validation case can be observed in Figure 2. As per the experiment [1], the flow speed for higher L/D was set for Mach 2.7, 4 and 6. Standard sea-level air conditions are modelled for the simulations with the parameters shown in Table 1.

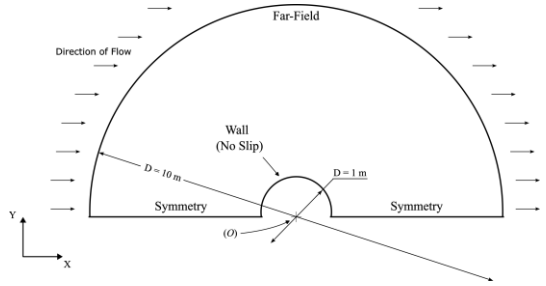

Fig 2: Schematics of boundary conditions used for the validation test case

Table 1 Initial freestream conditions for the present case

M_0	u	p	T	μ	ρ
2.7	926.1 m/s	101325 Pa	300 K	1.5689×10^{-5} N.s.m^{-2}	1.17662 kg/m^3
4	1372 m/s				
6	2058 m/s				

The flow regime in this case is mainly governed by compressible Navier-Stokes equations;

- Mass Continuity

$$\frac{\partial \rho}{\partial t} + \nabla \cdot (\rho \mathbf{U}) = 0 \quad (3.1)$$

- Momentum Continuity for Newtonian Fluid

$$\frac{\partial \rho \mathbf{U}}{\partial t} + \nabla \cdot [\mathbf{U}(\rho \mathbf{U})] - \nabla \cdot \mu \nabla \mathbf{U} = -\nabla p - \nabla \sigma \quad (3.2)$$

- Energy Equation for fluids, $e = C_v T$, with Fourie's Law $q = -k\nabla T$,

$$\frac{\partial \rho e}{\partial t} + \nabla \cdot (\rho \mathbf{U} e) - \nabla \cdot (\frac{k}{C_v}) \nabla e = p \nabla \cdot \mathbf{U} \quad (3.3)$$

- Ideal Gas Law

$$p = \rho R T \quad (3.4)$$

In the solution algorithm, we also incorporate the use of relaxation factors with the following values:

Table 2 Relaxation Factors

Relaxation Factors	Parameters	Values
Fields	U	0.6
	p	0.4
Equations involving the parameters	U	0.7
	k	0.7
	ϵ	0.7

Here the nature of the flow is determined by calculating the Reynold's number which shows the flow is turbulent. Thus, Standard K-epsilon turbulence model was used in this case. It is a Two transport equation linear-eddy-viscosity turbulence closure model where the two transport variables are turbulent kinetic energy, k and turbulent kinetic energy dissipation rate, ϵ.

The **turbulent kinetic energy** equation, k:

$$\frac{D}{Dt}(\rho k) = \nabla \cdot (\rho D_k \nabla_k) + P - \rho \epsilon \quad (3.5)$$

The **turbulent kinetic energy dissipation** rate equation, ϵ:

$$\frac{D}{Dt}(\rho \epsilon) = \nabla \cdot (\rho D_\epsilon \nabla_\epsilon) + \frac{C_1 \epsilon}{k}(P + C_3 \frac{2}{3} k \nabla . u) - C_2 \rho \frac{\epsilon^2}{k} \quad (3.6)$$

The **turbulent viscosity** equation, ν_t

$$\nu_t = C_\mu \frac{k^2}{\epsilon} \quad (3.7)$$

Further, the values for a few specific constants like C_μ, C_1, C_2, have been set according to standards. For calculating turbulent intensity (I), the formula for a fully developed pipe flow is used.

$$I = 0.16 \times Re^{(-\frac{1}{8})} \quad (3.8)$$

For our case, it will be around 0.034 ~ 3%. This is used to calculate various k and ϵ values for various velocities.

For isotropic turbulence, the turbulent kinetic energy can be estimated by:

$$k = \frac{3}{2}(I|\mathbf{u}_{\text{ref}}|)^2 \quad (3.9)$$

where, u_{ref} is reference flow speed.
For isotropic turbulence, the turbulence dissipation rate can be estimated by:

$$\epsilon = \frac{C_\mu^{0.75} k^{1.5}}{L} \quad (3.10)$$

where, C_μ is model constant equal to 0.09 by default.
L is reference length (m)

The 2D grid for the cylinder case has 60k hexahedral cells along with a grid independence study that has been conducted on Mach 2.7, as shown in Fig 3 and 4. For this study, five meshes were used and the size is reduced by the technique used by experts i.e., by doubling the mesh element count of the preceding courser mesh. Figure 4 shows the variation of the drag coefficient for the different meshes for the cylindrical domain.

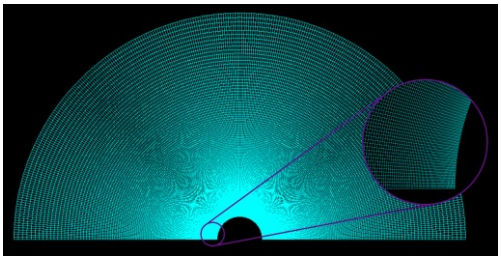

Fig 3. Mesh for the Cylinder Case

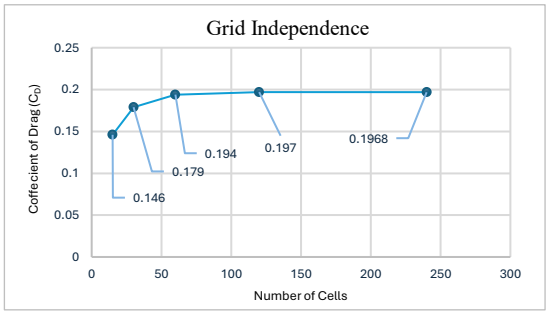

Fig 4: Grid Independence Plot for C_D vs number of cells.

Further, after the validation of Kim, and Chul-Soo's experimental results [1] using sonicFoam, we introduce the re-entry body geometries in the flow and analyze the aerodynamic and shock formation parameters. Figure 5 details the mesh characteristics of reentry vehicles.

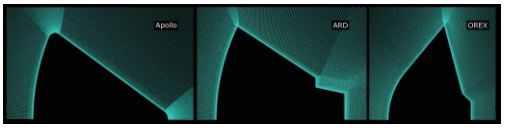

Fig 5: Mesh of re-entry bodies

4. VALIDATION AND RESULTS

4.1. Convergence Analysis

The residuals are one of the most fundamental measures of an iterative solution's convergence, as it directly quantifies the error in the solution of the system of equations. In a CFD analysis, the residual measures the local imbalance of a conserved variable in each control volume. Therefore, every cell in the model will have its own residual value for each of the equations being solved. Figure 4.1 shows the residuals of sonicFoam simulation at Mach number 2.7 representing that the simulation has attained a steady-state on time t = 0.02s plotted using pyFoam.

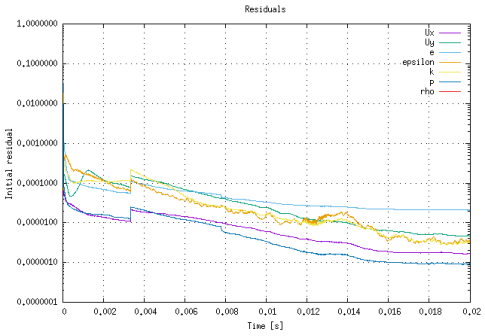

Fig 6: sonicFoam's Residual Plots

4.2. Literature Review

The interaction of shocks with solid obstacles is relevant in applications like high-speed flows with particles and hypervelocity impacts. Both experimental and analytical works are limited to simple geometries due to the nature of complexity in hypersonic flows [3]. Thus, computational studies are often looked at as alternatives. With recent advancements in computational techniques, several works were presented using DSMC, Navier-Fourier equations, and other analyses for high hypersonic flows over the Apollo capsule, considering effects like rarefaction and varying conditions [4, 5]. In the past, very limited work using OpenFOAM has been reported [6]. This article thus presents the comparison of supersonic flows using the OpenFOAM with the existing experiment [1]. The validation extends more with the comparison of isopycnics (contours of constant density) and streamlines where we show that sonicFoam overpredicts the density ratio (ρ/ρ_∞) at the windward side of the cylinder as shown in Figure 6. A similar overprediction can be seen in the pressure plot in Figure 8.

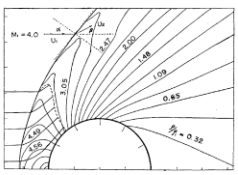

Kim, Chul-Soo's [1] Isopycnics, streamlines and sonic line

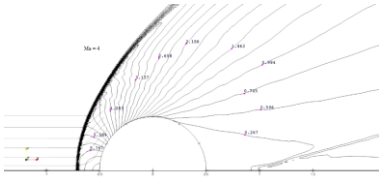

Validation plot for isopycnics and streamlines

Fig 6. Isopycnics and streamlines comparison at Mach 4

4.3. d/D and 1/b vs Mach number

The validation was conducted by comparing the plots in the experiment [1] with the existing results. Here, the d/D ratio is the ratio of shock stand-off distance (d) to the diameter of the cylinder (D). Figure 6 shows the relation between the d/D ratio and the inverse of 'b' and M_1 where 'b' can be expressed as, [1]

$$b = (D + 2d)/D$$

In simple terms, 'b' can be said to be the distance between the centre of the cylinder to the shock.

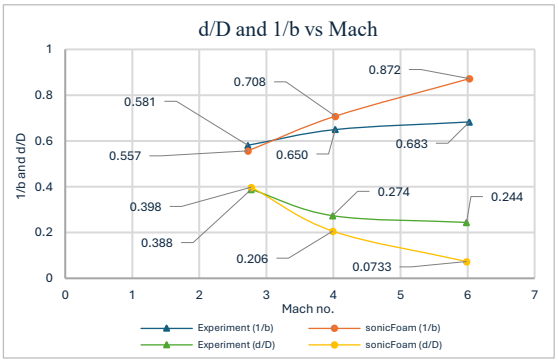

Figure 6: Comparison of d/D and 1/b vs Mach number with the experiment [1]

4.4. Pressure Distribution

Figure 7 details the pressure distribution over the cylinder, comparing various theories with reference experiments. The stagnation pressures for all velocities are higher than experimental values, while the pressures on the rearward side of the cylinder are lower. At $M_1 = 6$, the pressure drops rapidly after $\theta = 30°$, contrary to both experiments and theory. Implementing Sutherland's transport model for Mach 6 did not significantly change the results, highlighting the limitations of sonicFoam for hypersonic flows.

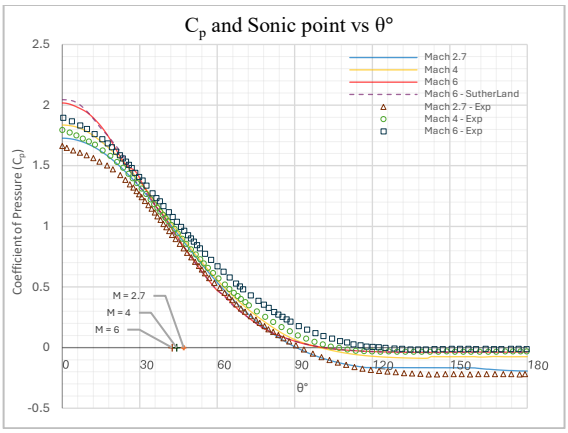

Figure 7: Validation for C_P vs θ°

4.5. Post Validation

Each of the re-entry bodies shows different behaviour in the flow due to their geometry. The reduction of shock stand-off distances is shown in Table 2.

Table 3 Freestream Values

Body	Mach no.	Shock Stand-off Distance (d)
Apollo	2.7	2.49 m
	4.0	1.46 m
	6.0	0.65 m
ARD	2.7	1.79 m
	4.0	1.12 m
	6.0	0.526 m
OREX	2.7	1.09 m
	4.0	0.669 m
	6.0	0.434 m

We further show for each body by varying the Mach number and plot the Mach number contours which show the velocity profiles over the bodies and further plot the Schlieren graphs which show the density gradient ($\nabla\rho$) to visualize the shock formation. We also analyze the drag estimation of the bodies.

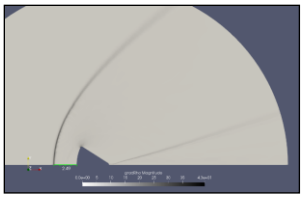

Schlieren Plot - Apollo

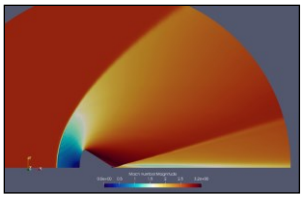

Mach contour - Apollo

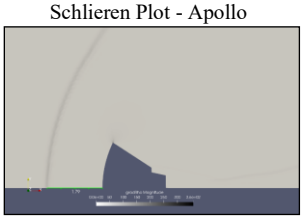

Schlieren Plot - ARD

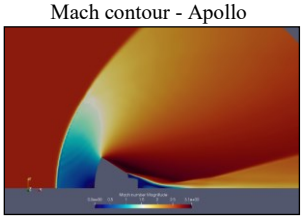

Mach contour - ARD

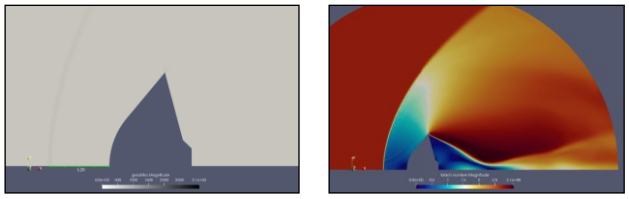

Schlieren Plot - OREX Mach contour - OREX

Figure 8: Contours for different re-entry bodies

The pressure distribution over the body for Apollo capsule can be shown below in Figure 9 in terms of pressure coefficients:

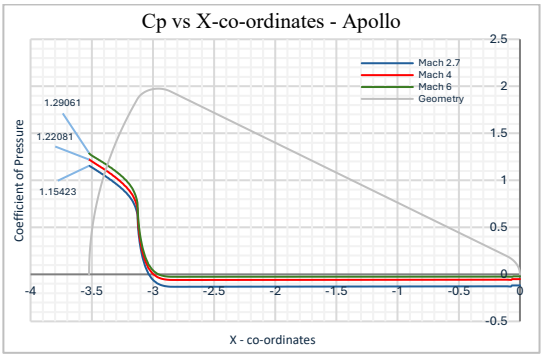

Fig 9: Pressure Distribution for the Apollo Capsule

Furthermore, the drag coefficients were calculated for each body at various Mach numbers shown in Table 4. From the values itself, we can observe major errors and inaccuracies while in the calculation of the drag for OREX and ARD bodies at M=6.

Table 4 Drag coefficients

Body	Mach number	Drag Coefficient (C_D)
Apollo	2.7	0.732
	4.0	0.725
	6.0	0.745
ARD	2.7	0.618
	3.35	0.611
	4.0	0.611
	6.0	8.038
OREX	2.7	0.710
	3.35	0.691
	4.0	0.668
	6.0	52.070

5. CONCLUSIONS

A numerical study was conducted to validate and investigate high-speed compressible turbulent flow over a blunt body. A validation was performed for the experimental results of Kim, and Chul Soo [1] by comparing various plots for the given Mach number flows. The study was further extended by implementing various re-entry capsules which were used by R.C. Mehta [2] in the flow and studying the effect of various Mach numbers which affects shock structure and Aerodynamic forces. We have also managed to conclude that 'sonicFoam', a pressure-based compressible openFoam solver lacks accuracy in the hypersonic regime wherein the solver couldn't compute the pressure distributions and shock structures with accurate results. A mesh independence study was also conducted and the least computationally expensive, yet accurate mesh size was determined. We further aim to investigate the re-entry shapes with axis-symmetric conditions to account for the 3D relaxation factors and analyze the heat fluxes over the bodies.

ACKNOWLEDGEMENT

The authors are thankful to the FOSSEE team and IIT Bombay, for their support. This case was a part of the 'Semester Long Internship' research migration project at FOSSEE, IIT Bombay.

REFERENCES

1. Kim[1], Chul-Soo[2] "Experimental Studies of Supersonic Flow past a Circular Cylinder". In: *Journal of the Physical Society of Japan Vol. 11, No. 4*, 1956
2. Mehta, R.C., "Numerical Computation of Heat Transfer on Reentry Capsules at Mach 5". In: *43rd AIAA Aerospace Sciences Meeting and Exhibit,* 2005.
3. Luther Neal Jr.[1] "Aerodynamic Characteristics at a mach number of 6.77of a 90° cone configuration, with and without spherical afterbodies, at angles of attack up to 180° with various degrees of nose blunting". In: *NASA TN D-1606,* 1963.
4. James, M., Christopher, G., and Francis, G., "DSMC simulations of Apollo capsule aerodynamics for hypersonic rarefied conditions." In *9th AIAA/ASME Joint Thermophysics and Heat Transfer Conference*, p. 3577. 2006.
5. Chourushi, T., Singh, S., Sreekala, V.A. and Myong, R.S., "Computational study of hypersonic rarefied gas flow over re-entry vehicles using the second-order Boltzmann-Curtiss constitutive model". *International Journal of Computational Fluid Dynamics*, 35(8), pp.566-593, 2021.
6. Mankodi, T.K., Ejtehadi, O., Chourushi, T., Rahimi, A. and Myong, R.S., "nccrFOAM suite: Nonlinear coupled constitutive relation solver in the OpenFOAM framework for rarefied and microscale gas flows with vibrational non-equilibrium." *Computer Physics Communications*, 296, p.109024, 2024.